

“© 2018 IEEE. Personal use of this material is permitted. Permission from IEEE must be obtained for all other uses, in any current or future media, including reprinting/republishing this material for advertising or promotional purposes, creating new collective works, for resale or redistribution to servers or lists, or reuse of any copyrighted component of this work in other works.”

Wideband Planarized Dual-Linearly-Polarized Dipole Antenna and Its Integration for Dual-Circularly-Polarized Radiation

Hai-Han Sun, *Student Member, IEEE*, He Zhu, Can Ding, *Member, IEEE*, and Y. Jay Guo, *Fellow, IEEE*

Abstract— A planarized dual-linearly-polarized (dual-LP) antenna and an integrated dual-circularly-polarized (dual-CP) antenna are proposed in this letter. For the dual-LP antenna, two groups of dipoles are fed by two balun-included feed networks to achieve $\pm 45^\circ$ polarizations. The feed networks and the radiators are printed on two sides of a substrate, forming a fully planar structure. Taking advantage of its planar configuration, the dual-LP antenna is further integrated with a wideband coupler to realize dual-CP radiation. The coupler is bent and squeezed into the space between the radiators and the reflector, leading to a compact structure. Both the dual-LP antenna and the dual-CP antenna have very stable radiation performances across a wide operating band $> 66\%$.

Index Terms— Dual-linear polarization, dual-circular polarization, integrated structure, stable radiation pattern, wideband.

I. INTRODUCTION

POLARIZATION diversity is a critical solution to minimize the multipath fading in a rich scattering environment. To that end, dual-linearly-polarized (dual-LP) antennas, especially $\pm 45^\circ$ -polarized antennas, and dual-circularly-polarized (dual-CP) antennas have been widely used in communication systems [1]. Wide bandwidth and stable radiation performances are desired for these antennas to support reliable high-data rate communications. Simple antenna configurations are preferred to reduce fabrication complexity and facilitate system integration.

Many wideband dual-LP antennas have been realized using dipole radiators [2]–[7], and their bandwidth can be greatly enhanced using tightly-coupled dipole arrays [8]. These designs normally have three main parts: dipole radiators, baluns, and reflectors. Balun, as a basic component to provide balanced feeding for dipoles, is always placed between the radiator and the reflector, occupying a large space. However, this space can be saved for system integration by replacing bulky and vertically placed baluns with planar ones. Some planar dual-LP antennas have been designed in [9], [10]. In [9], the feed network is printed on the same substrate with the

radiating dipoles. However, only one polarization was achieved with this configuration. In [10], an improved planar structure is realized using 180° hybrid couplers to provide differential feeds for dipoles, but the coupler inevitably adds design complexity. To the author's best knowledge, integrating baluns in a planar structure to realize dual-LP radiation has not been considered in literature so far.

Compared with wideband dual-LP antennas, wideband dual-CP antennas are more difficult to achieve, due to further bandwidth limitation by axial ratio (AR) performance. Recently, wideband dual-CP radiation have drawn ongoing attention by using patch antennas [11], [12], waveguide antennas [13]–[15], and frequency-independent antennas [16], [17]. However, most of the reported dual-CP antennas only have operating bandwidth less than 20% [12]–[15]. Wider bandwidth can be obtained using frequency-independent antennas such as log-periodic antenna [16] and sinuous antenna [17], which, however, suffer from complicated design and fabrication process, and require relatively large space.

In this paper, we propose a planar dual-LP antenna by integrating baluns on the same substrate as the dipole radiators. The circuit of the balun-included feed network is designed to facilitate the impedance matching within a restricted space. Stable radiation performance is achieved across a wide band from 1.55 GHz to 3.15 GHz with a planarized structure. This planarized structure can facilitate the system integration as RF components can be integrated into the space saved between the radiators and reflector for different purposes. As a demonstration, we integrate it with a wideband coupler to realize dual-CP radiation. Without occupying extra space, the antenna achieves stable dual-CP performance across a wide operating bandwidth over 80%.

II. THE PLANAR DUAL-LINEARLY-POLARIZED ANTENNA

The configuration of the fully planar $\pm 45^\circ$ dual-LP antenna is shown in Fig. 1. Four dipoles are arranged in a square and are printed on the bottom layer of the substrate. By simultaneously exciting dipoles 1 and 2, or dipoles 3 and 4, -45° - or $+45^\circ$ -polarized radiations can be realized. Two balun-included feed networks are designed and printed on the top layer of the substrate to match and feed the radiators. An 'air bridge' is used to avoid intersection between the two feed networks. The substrate used in this work is Rogers 4350B with a dielectric constant of 3.48 and a thickness of 1.524 mm. The antenna is

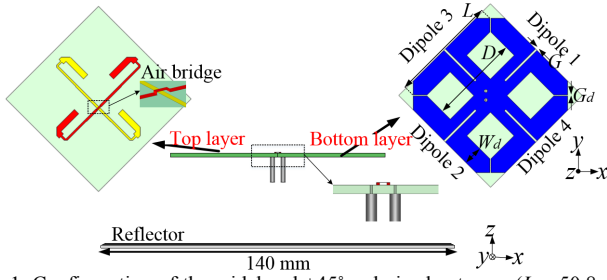


Fig. 1. Configuration of the wideband $\pm 45^\circ$ -polarized antenna. ($L = 50.8$ mm, $W_d = 9.24$ mm, $D = 42.4$ mm, $G_d = 0.59$ mm, $G = 1$ mm)

placed above a reflector with a distance of 35 mm.

The feed network for the proposed antenna needs to excite a pair of dipoles simultaneously and provide good impedance matching within a restricted space above the substrate. Fig. 2. (a) shows the circuit representation of the proposed feed network. As the dipoles are identical and have the same input impedance Z , the feed network is a duplication of the matching circuit for one dipole. The input impedance Z of each dipole is firstly transformed to 100Ω (Z') by an impedance matching circuit, and then connected in parallel to match to a standard $50\text{-}\Omega$ coaxial cable. The impedance matching circuit for each dipole consists of two transmission lines (TL_1 and TL_2), and a wideband balun formed by one open line (OL) and one short line (SL), as suggested in [18]. The feed networks were implemented using the microstrip structure, as shown in Fig. 2. (b), where only the feed network for dipoles 1 and 2 is shown for clarity. The SLs are realized by coupled lines connecting the dipoles to a rectangular patch located at the center of the board. The OL and TLs are microstrip lines printed on the top layer of substrate. The dipoles, SLs, and the shorting patch also act as the ground for the OL and TLs. A $50\text{-}\Omega$ coaxial cable with its inner conductor connected to the intersection of the two TL_1 s on the top layer, and its outer conductor soldered with the patch on the bottom layer is used to feed the antenna. The optimized parameters for the feed network are listed in Table I.

The impedances of dipole before and after adding the impedance matching structure, and the S-parameters before and after implementing the feed network are shown in Fig. 3. As shown in Fig. 3. (a), before adding the impedance matching structure, the impedance of dipole Z has a large capacitance value around $-50j \Omega$, and a relatively small resistance value around 60Ω across a wide band. After adding the impedance matching structure, the impedance of dipole Z' is transformed to 100Ω with reactance value around 0. Two Z' can be connected in parallel and fed by a 50Ω port. The resultant S-parameters before and after adding the feed network are plotted in Fig. 3. (b). The dipoles cannot be matched without the feed network, but are well-matched to $|S_{11}| < -10$ dB from 1.55 GHz to 3.0 GHz after implementing the feed network, demonstrating the effectiveness of the planar feed network in impedance matching.

The prototype of the dual-LP antenna was fabricated and tested, as shown in Fig. 4. Plastic posts are used to support the antenna. The simulated and measured S-parameters of the two

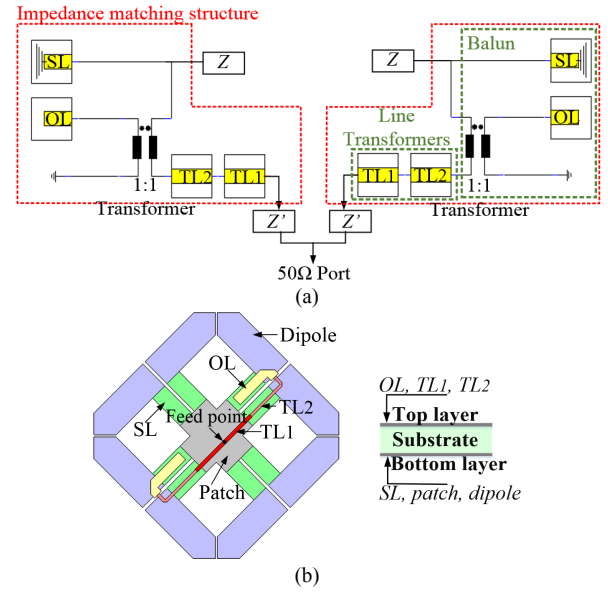


Fig. 2. (a) Circuit representation, and (b) physical realization of the feed network.

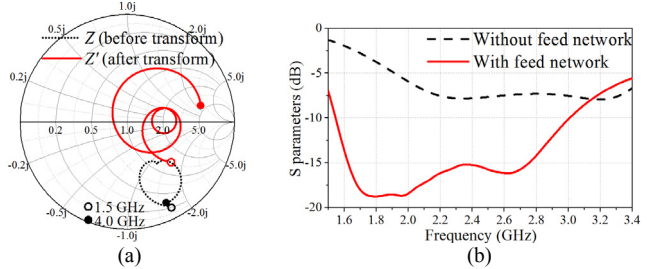


Fig. 3. (a) Smith Chart of the dipole impedance before and after the impedance matching structure. (b) S-parameters before and after adding the feed network.

Elements	Line length	Line width	Gap width
TL_1	11.44 mm	1.1 mm	-
TL_2	15.10 mm	0.9 mm	-
OL	13.10 mm	2.9 mm	-
SL	11.50 mm	5.0 mm	1.0 mm

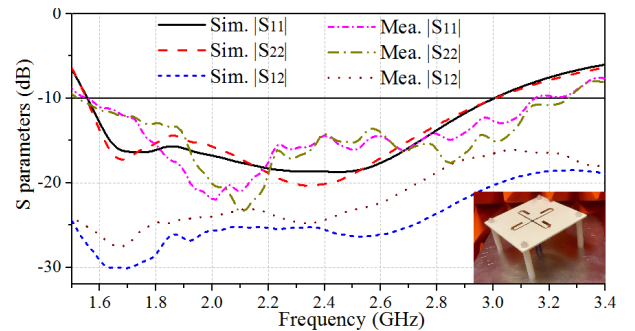


Fig. 4. Simulated and measured S-parameters of the dual-linearly-polarized antenna.

ports are also shown in Fig. 4. The measured bandwidth is 68% from 1.55 GHz to 3.15 GHz. Across this wide band, the measured port isolation is > 17 dB. The simulated and measured radiation patterns for $+45^\circ$ polarization in xoz -plane at 1.7 GHz, 2.2 GHz, and 2.7 GHz are given in Fig. 5. The

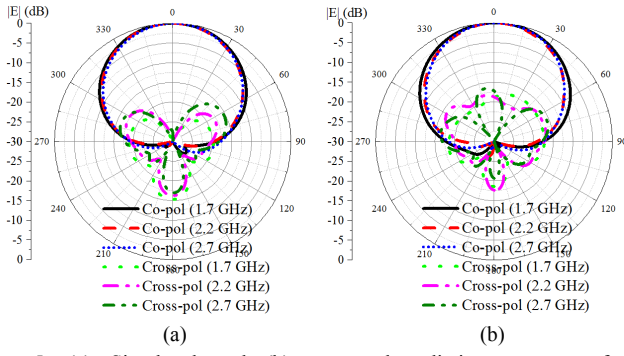


Fig. 5. (a) Simulated and (b) measured radiation patterns of the dual-linearly-polarized antenna at 1.7 GHz, 2.2 GHz, and 2.7 GHz.

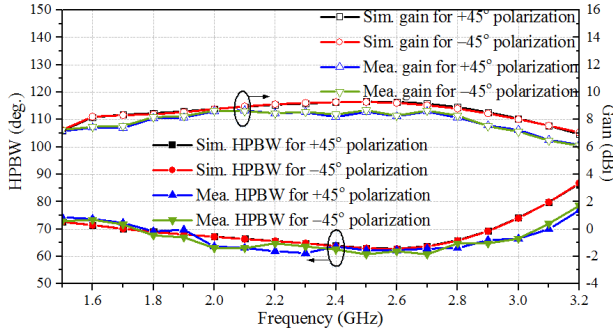


Fig. 6. Simulated and measured HPBW and gain of the dual-linearly-polarized antenna.

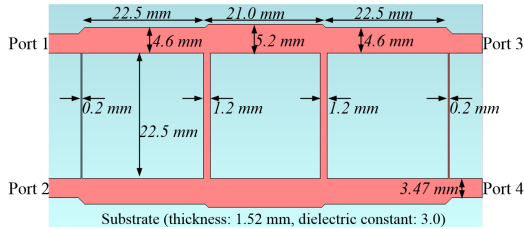


Fig. 7. The layout of the wideband quadrature coupler.

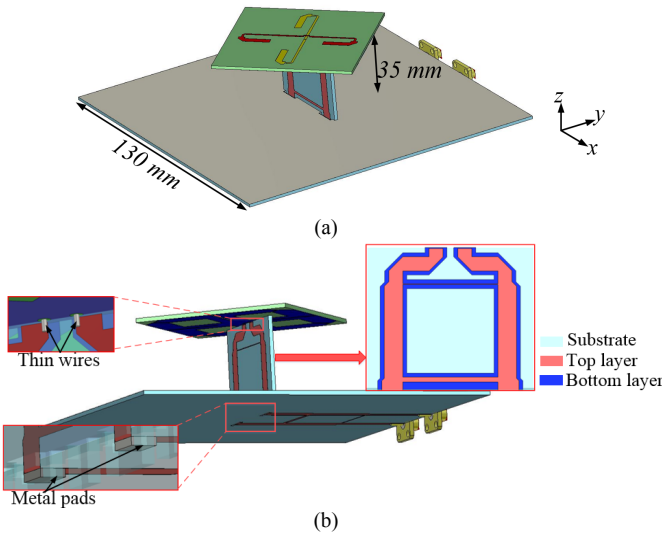


Fig. 8. (a) Top and (b) bottom perspective views of the dual-CP antenna.

measured results agree well with the simulated ones, and both demonstrate stable boresight radiation properties. The measured cross-polarization discrimination (XPD) is > 16 dB. Fig. 6 shows the half-power-beamwidth (HPBW) and gain

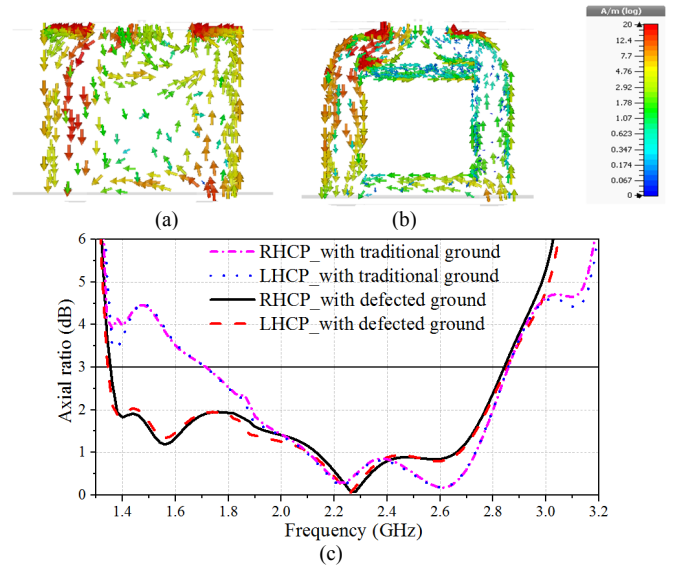


Fig. 9. Current distribution on the coupler with (a) a traditional ground and (b) a defected ground, and (c) the axial ratio for the two cases.

performances. The measured horizontal HPBW varies within $67.5^\circ \pm 6.5^\circ$ for the two polarizations across the operating band. The simulated and measured gain varies from 8.0 dBi to 9.3 dBi, and from 6.5 dBi to 8.7 dBi, respectively. The discrepancy between them is mainly attributed to the losses from coaxial cables.

III. THE INTEGRATED DUAL-CIRCULARLY-POLARIZED ANTENNA

A. Configuration of the Dual-Circularly-Polarized Antenna

By creating $+90^\circ$ and -90° phase differences while maintaining equal magnitude between two input ports of a orthogonal dual-LP antenna, dual-circular polarization can be realized. In this work, a quadrature coupler is integrated with the planar dual-LP antenna to achieve dual-CP radiation.

Firstly, a traditional three-section branch-line coupler is designed, as shown in Fig. 7. When Port 1 or Port 2 is excited, the output signals at Port 3 and Port 4 have a 90° or -90° phase difference, respectively, with balanced magnitudes from 1.42 GHz to 3.0 GHz. The wideband coupler is then integrated with the designed dual-LP antenna to realize desired dual-CP radiation. Although the coupler has a large dimension, it can be bent to optimally fit in the space saved by the planar-configured dual-LP antenna, as shown in Fig. 8. Part of the coupler is placed between the antenna aperture and the reflector, providing mechanical support. The other part of the coupler is located on the other sides of the reflector. After being integrated with the bent coupler, the reflector becomes a printed circuit board with one side all covered with metal functioning as reflector and the other side printed with microstrip lines. For the vertical part of the coupler, instead of using a traditional ground fully covered by metal, a defected ground is adopted, as shown in Fig. 8. (b). Most of metal of the ground is removed except the metal at the back of microstrip lines, making the ground appear as a zoomed-out coupler. The reason for modifying the ground is to minimize its negative effect on the antenna's AR performance. Fig. 9 shows the current distribution and the



Fig. 10. Prototype of the dual-circularly-polarized antenna.

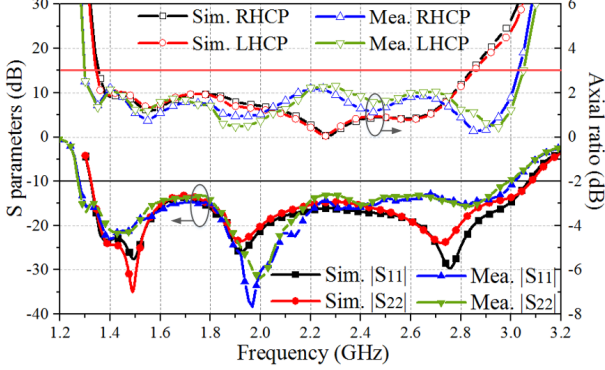


Fig. 11. Simulated and measured S-parameters and axial ratios of the dual-circularly-polarized antenna.

resultant AR performance with the traditional and defected grounds, respectively. As shown in Fig. 9. (a), a considerable amount of currents are distributed in the edges and middle of the traditional ground, which significantly deteriorates the AR performance shown in Fig. 9. (c). By adopting the defected ground, the currents concentrate on the back of the microstrip line, as shown in Fig. 9. (b), thereby introducing minimal deterioration to AR. With the defected ground, AR is maintained < 2 dB from 1.4 GHz to 2.75 GHz.

The connections between the antenna aperture, the vertical part of coupler, and the reflector are carefully designed. On the upper part, the ground of the coupler is directly attached to the middle patch on the radiator layer, and the microstrip lines is connected with the feed lines on the top layer using thin wires. On the lower part, the reflector is etched with some slots to insert the vertical coupler in. Additional metal pads are utilized to ensure good connection between the microstrip lines on the vertical and horizontal parts of the coupler.

B. Simulated and Measured Results

The dual-CP antenna is also fabricated and tested, as shown in Fig. 10. When ports 1 or 2 is excited, left-handed circular polarization (LHCP) or right-handed circular polarization (RHCP) radiation is obtained. The simulated and measured reflection coefficients and AR results of the two circular polarizations are shown in Fig. 11. The simulated and measured 10-dB impedance bandwidth for the two ports are 79.7% and 81%, respectively. The measured 3-dB AR bandwidth is 80% from 1.3 GHz to 3.04 GHz. The radiation patterns for RHCP at 1.5 GHz, 2.2 GHz and 3.0 GHz are shown in Fig. 12. As the radiation patterns for LHCP are very similar to those of the RHCP, they are not shown here for brevity. The measured patterns agree well with the simulated ones, and both demonstrate good broadside CP radiations. The HPBW and gain results for the two polarizations are shown in Fig. 13. The gain is very stable across most of the operation band, with a

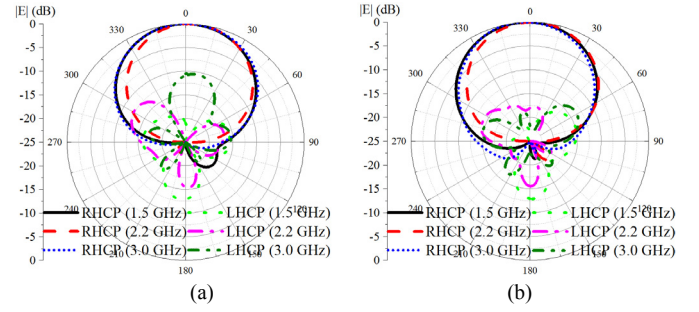


Fig. 12. (a) Simulated and (b) measured radiation patterns of RHCP at 1.5 GHz, 2.2 GHz, and 3.0 GHz.

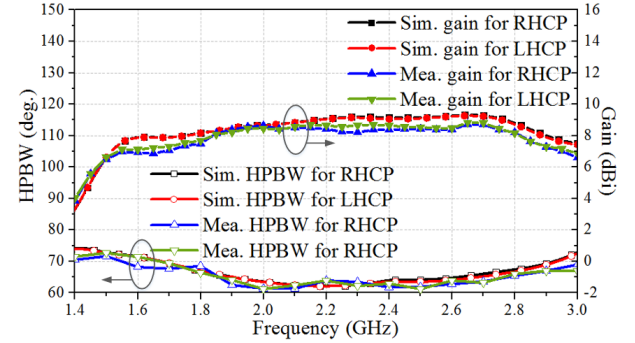


Fig. 13. Simulated and measured HPBW and gain of the dual-circularly-polarized antenna.

TABLE II
COMPARISON OF DUAL-CP ANTENNAS' PERFORMANCE

Ref.	Antenna size (λ^3)	Bandwidth*	Maximum gain (dBi)
[12]	0.76*0.76*0.22	13.0%	4.9
[15]	5.44*2.69*0.54	11.8%	10.3
[17]	1.17*1.17*1.75	85.7%	7.5
This work	0.95*0.95*0.26	80%	9.3

* The criteria for the operating band is reflection coefficients < -10 dB and AR < 3 dB.

peak of 9.3 dBi at 2.7 GHz. The overlapped bandwidth of -10 -dB reflection coefficient, 3-dB AR, and 3-dBi gain variation is 66.7% from 1.50 GHz to 3.0 GHz. Across this wide band, the radiation pattern is very stable with the horizontal HPBW varies within $67.5^\circ \pm 5^\circ$. Table II lists the comparison of this work and previous published wideband dual-CP antenna elements. It shows that this antenna has a wideband and high-gain performance with a relatively compact size.

IV. CONCLUSION

A fully planar dual-LP antenna comprising four concentrically arranged dipoles has been proposed. For the first time, baluns are included in the feed network for the planarized dual-LP antennas. With a simple and compact structure, the antenna has stable radiation performances across a wide bandwidth of 68%. Based on the dual-LP antenna structure, a dual-CP antenna is realized by integrating a wideband coupler into the space between the radiators and reflector. The dual-CP antenna has a wide overlapping bandwidth of 66.7% for 10-dB impedance coefficient, 3-dB AR, and 3-dBi gain variation with very stable radiation performances. The proposed design serves as good candidates and offers a direction for future integrated antenna systems.

REFERENCES

- [1] A. Dastranj, "Low-profile ultra-wideband polarisation diversity antenna with high isolation", *IET Microw. Antennas Propag.*, vol. 11, iss. 10, pp. 1363-1368, Aug. 2017.
- [2] H. Huang, Y. Liu, and S. Gong, "A broadband dual-polarized base station antenna with sturdy construction," *IEEE Antennas Wireless Propag. Lett.*, vol. 16, pp. 665-668, 2017.
- [3] Z. Bao, Z. Nie, and X. Zong, "A novel broadband dual-polarization antenna utilizing strong mutual coupling," *IEEE Trans. Antennas Propag.*, vol. 62, no. 1, pp. 450-454, Jan. 2014.
- [4] C. Ding, H. Sun, R. W. Ziolkowski and Y. J. Guo, "Simplified tightly-coupled cross-dipole arrangement for base station applications," *IEEE Access*, vol. 5, pp. 27491-27503, Nov. 2017.
- [5] Y. H. Huang, Q. Wu, and Q. Z. Liu, "Broadband dual-polarized antenna with high isolation for wireless communication," *Electron. Lett.*, vol. 45, no. 14, pp. 714-715, July 2009.
- [6] S. G. Zhou, P. K. Tan, and T. H. Chio, "Low-profile, wideband dual-polarized antenna with high isolation and low cross polarization," *IEEE Antennas Wireless Propag. Lett.*, vol. 11, pp. 1032-1035, 2012.
- [7] H. Sun, C. Ding, B. Jones and Y. J. Guo, "A wideband base station antenna element with stable radiation pattern and reduced beam squint," *IEEE Access*, vol. 5, pp. 23022-23031, Oct. 2017.
- [8] D. K. Papantonis and J. L. Volakis, "Dual-polarized tightly coupled array with substrate loading," *IEEE Antennas Wireless Propag. Lett.*, vol. 15, pp. 325-328, 2016.
- [9] Y. H. Cui, R. L. Li, P. Wang, "A novel broadband planar antenna for 2G/3G/LTE base stations", *IEEE Trans. Antennas Propag.*, vol. 61, no. 5, pp. 2767-2774, May 2013.
- [10] Y. Cui, X. Gao, and R. Li, "A broadband differential fed dual-polarized planar antenna", *IEEE Trans. Antennas Propag.*, vol. 65, iss. 6, pp. 3231-3234, June 2017.
- [11] R. Xu, J. -Y. Li, J. Liu, S. -G. Zhou, k. Wei, and Z. -J. Xing, "A simple design of compact dual-wideband square slot antenna with dual-sense circularly polarized radiation for WLAN/Wi-Fi Communications," *IEEE Trans. Antennas Propag.*, Early access, June 2018.
- [12] Q. Luo, S. Guo, and L. Zhang, "Wideband multilayer dual circularly-polarised antenna for array application," *Electron. Lett.*, vol. 51, no. 25, pp. 2087-2089, Dec. 2015.
- [13] J. Wu, Y. J. Cheng, H. B. Wang, Y. C. Zhong, D. Ma, and Y. Fan, "A wideband dual circularly polarized full-corporate waveguide array antenna fed by triple-resonant cavities," *IEEE Trans. Antennas Propag.*, vol. 65, no. 4, pp. 2135-2139, Apr. 2017.
- [14] S. -G. Zhou, G. -L. Huang, and T. -H. Chio, "A lightweight, wideband, dual-circularly-polarized waveguide cavity array designed with direct metal laser sintering considerations," *IEEE Trans. Antennas Propag.*, vol. 66, no. 2, pp. 675-682, Feb. 2018.
- [15] Y. Cai, Y. Zhang, Z. Qian, W. Cao, and S. Shi, "Compact wideband dual circularly polarized substrate integrated waveguide horn antenna," *IEEE Trans. Antennas Propag.*, vol. 64, no. 7, pp. 3184-3189, Apr. 2016.
- [16] R. Sammeta, and D. S. Filipovic, "Reduced size planar dual-polarized log-periodic antenna for bidirectional high power transmit and receive applications," *IEEE Trans. Antennas Propag.*, vol. 62, no. 11, pp. 5453-5461, Nov. 2014.
- [17] S. Zheng, et al. "A broadband dual circularly polarized conical four-arm sinusoidal antenna," *IEEE Trans. Antennas Propag.*, vol. 66, no. 1, Jan. 2018.
- [18] C. Ding, B. Jones, Y. J. Guo and P. Y. Qin, "Wideband matching of full-wavelength dipole with reflector for base station," *IEEE Trans. Antennas Propag.*, vol. 65, no. 10, pp. 5571-5576, Oct. 2017.